

Article

Effect of Different Power Supply Modes on Inclusion in 304L Stainless Steel Electroslag Ingot

Xiaofang Shi, Bingjie Wang, Yu Wang and Lizhong Chang *

School of Metallurgy Engineering, Anhui University of Technology, Ma'anshan 243002, China

* Correspondence: clz1997@163.com

Abstract: The use of low frequency or DC (i.e., direct current) operation in the electroslag remelting process may lead to the electrolysis of some oxides in the slag pool, which will adversely affect the cleanliness of the electroslag ingot. In order to confirm this view, the effect of different power supply modes on the oxygen content and inclusions in electroslag ingot has been studied by adopting the self-designed electroslag remelting furnace as experimental equipment. The pulse heating inert gas fusion-infra-red absorption method is used for analyzing oxygen content. The analysis of non-metallic inclusion is conducted using an automatic SEM (i.e., scanning electron microscope) made by the American ASPEX Company, where the inclusion type and the inclusion size are determined. Results show that the oxygen content in the electroslag ingot increase significantly compared with that in the consumable metal electrode, whether under the frequency of 50 Hz, low-frequency, or DC. When DCSP (i.e., the consumable electrode is connected to the cathode of the DC power supply), DCRP (i.e., the consumable electrode is connected to the anode of the DC power supply), 2 Hz, 10 Hz, and 50 Hz power supply modes are adopted, the oxygen content in electroslag ingot is 155.3 ppm, 100.4 ppm, 75.8 ppm, 66.3 ppm, and 43.2 ppm respectively. With the increase in oxygen content, the number of inclusions in electroslag ingots increases significantly, and the increased inclusions are mainly Al_2O_3 inclusions. Regardless of the power supply mode, the largest diameter of inclusion is less than 20 μm . The electrolysis of Al_2O_3 is the direct reason for the increase in oxygen in the electroslag ingot when $CaF_2-Al_2O_3$ slag is used. With the decrease in frequency, the electrolysis trend increases, and the oxygen content and the number of inclusions also increase. However, most of the inclusions are regenerated with the decrease in metal pool temperature and solidification, so the size is fine.



Citation: Shi, X.; Wang, B.; Wang, Y.; Chang, L. Effect of Different Power Supply Modes on Inclusion in 304L Stainless Steel Electroslag Ingot. *Metals* **2023**, *13*, 457. <https://doi.org/10.3390/met13030457>

Academic Editor: Mark E. Schlesinger

Received: 5 January 2023

Revised: 4 February 2023

Accepted: 20 February 2023

Published: 22 February 2023



Copyright: © 2023 by the authors. Licensee MDPI, Basel, Switzerland. This article is an open access article distributed under the terms and conditions of the Creative Commons Attribution (CC BY) license (<https://creativecommons.org/licenses/by/4.0/>).

Keywords: electroslag remelting; low-frequency; DC; oxygen; inclusion; electrolysis

1. Introduction

The single-phase power supply with a frequency of 50 Hz is the most important power supply mode for an electroslag furnace, including the single electrode, bifilar, and coaxial conduction electroslag furnace. This power supply mode has been widely used in the electroslag remelting process because of its convenient operation and simple equipment. However, the single-phase and power supply mode with a frequency of 50 Hz has very great electrical defects. In the process of electroslag remelting, the large current output from the transformer forms a strong magnetic field that increases the resistance and inductive reactance of the short network and results in an increase in the voltage loss and the decrease in power factor, which will increase the consumption of electricity per ton steel [1]. Especially when single electrode operation is adopted, the power factor is generally only approximately 0.62–0.80. In addition, the single-phase power supply mode with a frequency of 50 Hz increases the three-phase imbalance of the power system and leads to serious harmonic pollution [2,3].

To overcome the disadvantages of single-phase power supply modes with a frequency of 50 Hz, low-frequency power supply, as a new power supply mode, has attracted the attention of metallurgists, and numerous basic research has been carried out [4–9]. With the

decrease in power frequency, the electrical efficiency increases, and the three-phase balance of the power system can be proved. In addition to low frequency, DC power is occasionally introduced into the electroslag process, which is conducive to the improvement of electrical efficiency. Although the low-frequency and DC operations have electrical advantages, metallurgists pay more attention to their influence on the metallurgical quality of electroslag ingot. Wang, Q et al. [10] analyze the effect of DC electroslag remelting on desulfurization by numerical simulation and find the desulfurization ratio of DCRP is significantly higher than that of DCSP. Through experimental research, Aksenov, I.A et al. [11] find that compared with DC electroslag remelting, AC electroslag remelting has the highest desulfurization rate, followed by DCRP, and DCSP has the worst desulfurization effect. However, the changes in oxygen content and inclusions are not mentioned in the above studies. With the development of modern secondary refining technology, the sulfur in the consumable electrode can be easily removed in large quantities. Therefore, metallurgists are more concerned about the change of oxygen and inclusions in the electroslag ingot caused by the power supply mode. Armin Parr et al. [12,13] find that the distribution of different kinds of inclusions in electroslag ingot is closely related to the power supply mode. Alec Mitchell discusses the electrochemical aspects of the low-frequency and DC electroslag process, but no more data on the oxygen and inclusions in electroslag ingots have been provided [14]. In a previous study, authors found that when the power frequency is decreased, the oxygen content in the electroslag ingot is significantly increased [15,16]. To further study the influence of low-frequency and DC power supply mode on the cleanliness of electroslag ingot, the electroslag remelting experiments are carried out using 304L stainless steel as the research object based on the laboratory-scale experiment. The variation of oxygen and inclusion in electroslag ingot prepared with different power supply modes are studied in detail.

2. Experimental Section

2.1. Experimental Equipment

The experiment is carried out on the laboratory-scale electroslag furnace, as shown in Figure 1. A 100 kVA AC power supply (50 Hz) is available for the preparation of electroslag ingots with a diameter of 50–120 mm, with a high voltage terminal of 380 V, a low voltage terminal that ranges from 28–40 V, and a maximum current of 2500 A. The frequency conversion unit is installed at the low-voltage terminal of transformer. The main circuit of frequency conversion unit is composed of two reverse parallel single-phase bridge thyristor rectifiers. By adjusting the length of the alternating conduction time of two rectifier circuits, the output frequency can be adjusted between 0–10 Hz, either low-frequency output or DC output. By adjusting the conduction angle of thyristor, the output voltage could be adjusted continuously between 0 and the output voltage of transformer. The output end of frequency conversion unit is connected to the consumable electrode and cooled copper baseplate. During the remelting process, the voltage and frequency are fixed, and the current can reach the set value by adjusting the moving speed of consumable electrode manually.

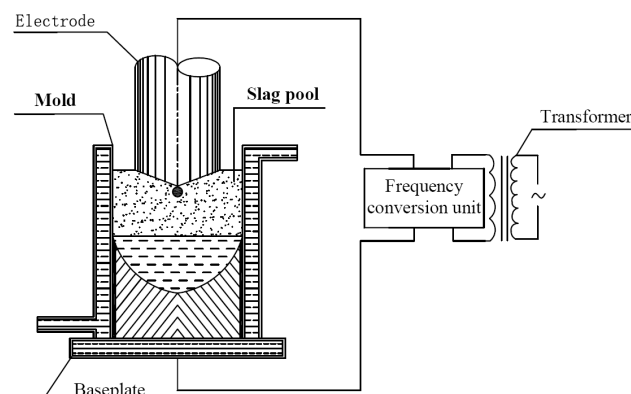


Figure 1. Low-frequency (DC) electroslag remelting furnace.

The waveform shown in Figure 2 can be obtained through the rectification of the frequency conversion unit.

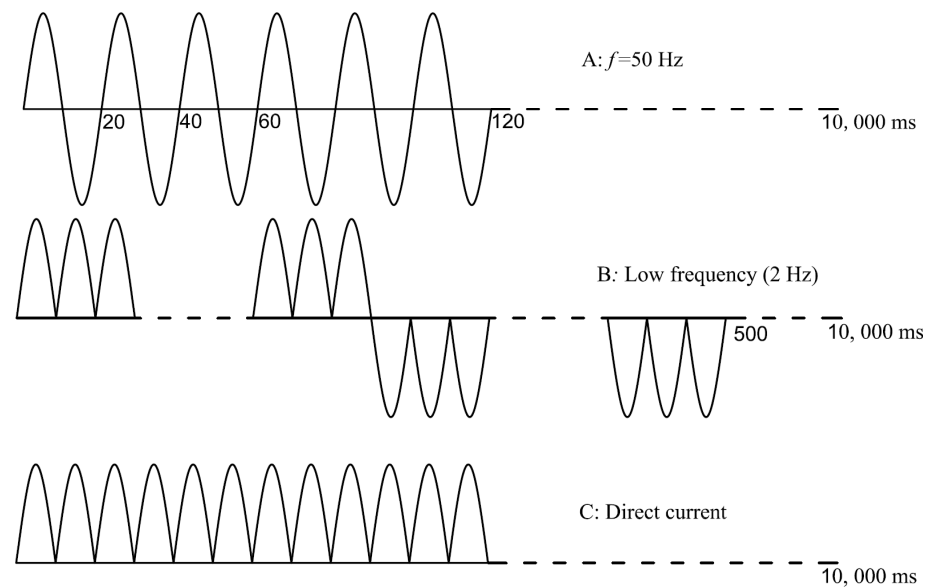


Figure 2. Waveform of different power supply modes.

2.2. Feedstock

The 304L austenitic stainless steel used in the experiment is prepared by 30 t EAF-AOD-LF-CC process and then forged into the consumable metal electrode. The compositions of electrode are shown in Table 1.

Table 1. Chemical compositions of the electrode material.

Elements	C	Si	Mn	P	S	Ni	Cr	Al	O
wt%	0.019	0.41	1.18	0.037	0.0025	8.10	18.27	0.010	0.0025

The traditional slag that contains 30 wt%Al₂O₃-70 wt%CaF₂ is used for the electroslag remelting experiment, where Al₂O₃ and CaF₂ are prepared by Sinopharm Chemical Reagent Co., Ltd. The height of slag pool during remelting is about 50 mm (1200 g slag).

2.3. Experimental Parameters and Testing

A mold with an upper diameter of 95 mm, a bottom diameter of 105 mm (cone-shaped), and a height of 250 mm is adopted. The diameter of consumable metal electrode is 50 mm. The scale in electrode surface is removed by grinding prior to electroslag remelting. No deoxidizer is added to the slag bath during the electroslag remelting process. The pressure of cooling water is between 0.2 MPa and 0.3 MPa. All ingots are remelted in the atmospheric environment.

Hot start is adopted for electroslag remelting. First, Al₂O₃ and CaF₂ are mixed and placed into a graphite crucible. Then, the graphite crucible is placed into a high-temperature furnace at 1600°C for melting. After completely melting the slag, it is quickly taken out and poured into the mold. The consumable electrode drops, and remelting begins.

In the previous study, the authors analyze the influence of power supply frequency (50 Hz, 2 Hz, 1 Hz, 0.4 Hz, 0.1 Hz) on the cleanliness of electroslag ingots in detail [16]. In order to further clarify the influence of frequency on cleanliness, in addition to low-frequency electroslag remelting, the DC electroslag remelting is supplemented in this paper, and the experimental schemes are shown in Table 2.

Table 2. Experimental schemes.

Experimental Schemes	Remelting Current/A	Remelting Voltage/V	Power Frequency/Hz	Power Cycle/s
1	1400	20	10	0.1
2	1400	20	2	0.5
3	1400	20	DCSP *	
4	1400	20	DCRP **	
5	1800	28	50	0.02

* Consumable electrode is connected to cathode of DC power supply; ** Consumable electrode is connected to anode of DC power supply.

After remelting, the samples of 15 mm × 15 mm × 15 mm and \varnothing 5 mm × 100 mm are cut off at 30 mm below the upper part of the electroslag ingot for inclusion and oxygen content analysis. The analysis of non-metallic inclusion is carried out with an automatic SEM made by American ASPEX Company, where the inclusion type and size are determined at an area of approximately 60 mm². JSM-6510LV SEM is used to further analyze the distribution of elements in inclusion. After the surface of sample of \varnothing 5 mm × 100 mm is polished, the oxygen content is tested at three different positions of the sample, and the average value of oxygen content at different positions is used as the final oxygen content in electroslag ingot. In this paper, the pulse heating inert gas fusion-infrared absorption method is used to determine the oxygen content. Ca content is analyzed by inductively coupled plasma-atomic emission spectrometry (ICP-AES), and others are analyzed by electric spark direct reading spectrometry.

3. Experimental Results and Analysis

3.1. Variation of Oxygen Content in Electroslag Ingot with Different Power Supply Modes

Figure 3 shows the oxygen content in electroslag ingots with the frequency of 2 Hz, frequency of 50 Hz, and DC operation. For comparison, the oxygen content in the electrode is presented in Figure 3.

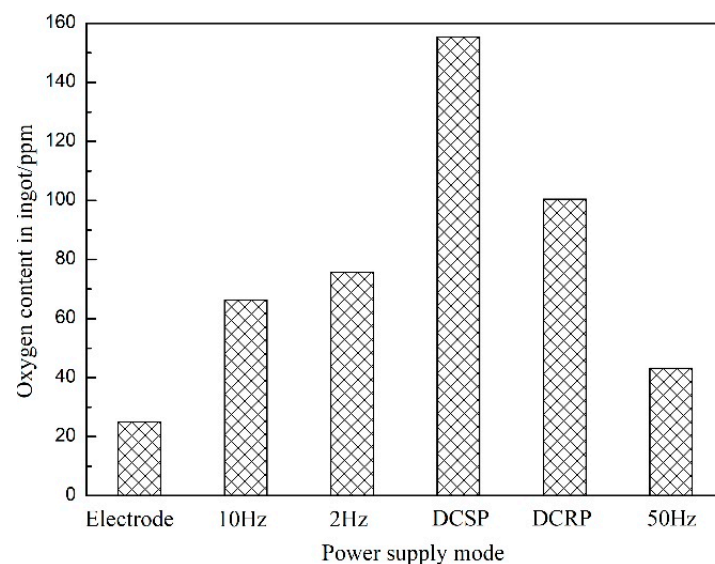
**Figure 3.** Oxygen content in ingots with different power supply modes.

Figure 3 shows that regardless of power supply modes, the oxygen content in the electroslag ingot increases compared with that in the consumable electrode. However, the increase in oxygen obviously varies with different power supply modes. When the power frequency is 50 Hz, the oxygen content in the electroslag ingot increases to 43.2 ppm from 25 ppm in the consumable electrode. The oxygen contents with power frequencies of 10 Hz

and 2 Hz are 66.3 ppm and 75.8 ppm, respectively. When DCRP is used for power supply, the oxygen content increases to 100.4 ppm. When DCSP is used, the oxygen content sharply increases to 155.3 ppm.

The above data suggest that the power supply mode has a very important effect on the oxygen content in the electroslag ingot, and the order of its influence on oxygen content is DCSP, DCRP, frequency of 2 Hz, and frequency of 50 Hz.

3.2. Inclusions in Electroslag Ingots with Different Power Supply Modes

In order to analyze the effect of power supply mode on the inclusion in electroslag ingot, the number, type, and size distribution of inclusions in 304 L stainless steel ingot are analyzed by an automatic SEM.

3.2.1. Number and Size of Inclusions

Figure 4 shows the distribution of inclusions with different sizes in electroslag ingots prepared with various power supply modes, where the equivalent cycle diameter is used. The figure shows that only 356 inclusions are in consumable electrodes because of the low oxygen content. When the power frequency is 50 Hz, the number of inclusions in the electroslag ingot increases to 758. When the frequencies are 10 Hz and 2 Hz, the number of inclusions is 1166 and 1241, respectively. When DCRP mode is adopted, the number of inclusions is similar to that at 2 Hz. When the DCSP mode is adopted, the number of inclusions increases to more than 2500. The variation rule of the number of inclusions is consistent with that of the oxygen content in Figure 3.

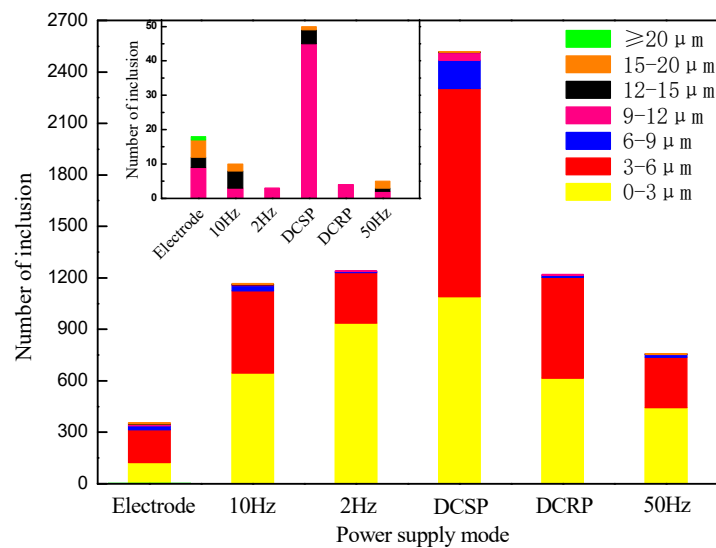


Figure 4. Effect of Power supply mode on number and size of inclusion.

Figure 4 also shows that regardless of the power supply modes, the diameter of most inclusions is less than 6 μm, and the maximum diameter is less than 20 μm. However, the maximum diameter of inclusions in the consumable electrode is 27.4 μm. In terms of the number of inclusions, except for DCSP, the number of large inclusions with a diameter greater than 9 μm at other power supply modes is less than that in consumable electrodes.

3.2.2. Inclusion Type

Power supply modes affect not only the number and size of inclusions but also the types of inclusions, as shown in Figure 5.

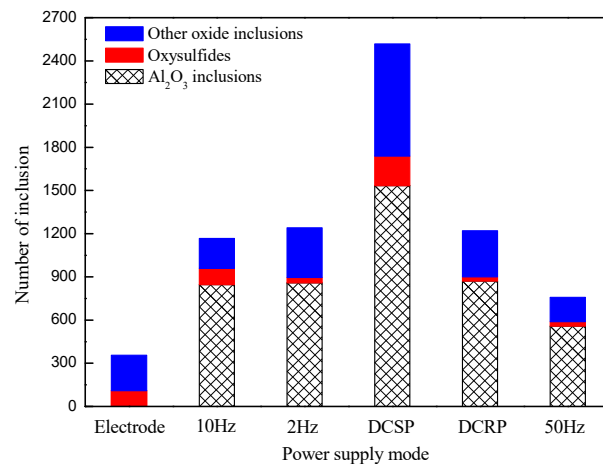
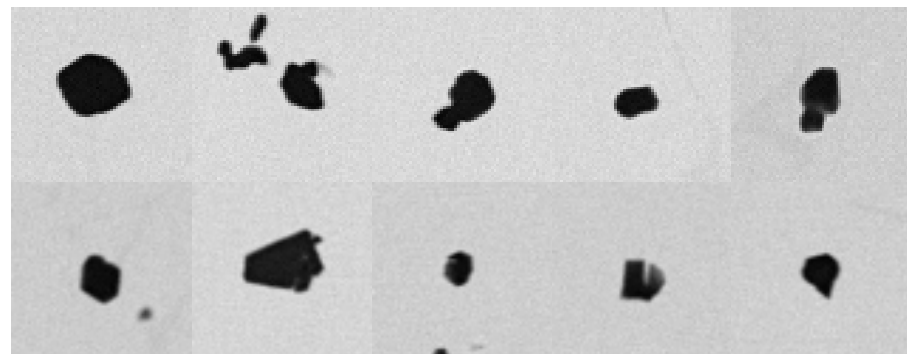
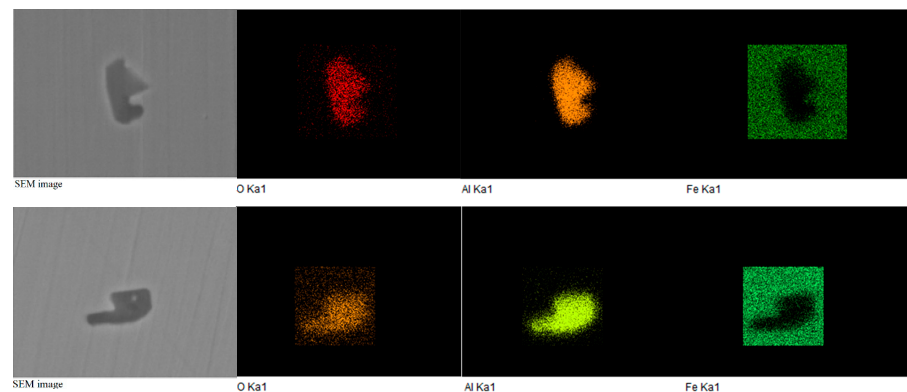


Figure 5. Effect of Power supply mode on inclusion type.

Figure 5 shows that the inclusions in the electroslag ingot are mainly Al_2O_3 , followed by other composite oxides and oxysulfides. Because the sulfides in electroslag ingots are few, they are not listed separately. Due to the use of calcium treatment technology in the smelting process of consumable electrodes, there are almost no Al_2O_3 inclusions in consumable electrodes. The power supply modes have a significant effect on the number of Al_2O_3 in the electroslag ingot. With the decrease in power supply frequency, the number of Al_2O_3 inclusions gradually increases, and when DCSP mode is adopted, the number of Al_2O_3 is the largest. Figure 6 presents the SEM-EDS diagram of Al_2O_3 inclusions.



(a)



(b)

Figure 6. SEM-EDS image of Al_2O_3 . (a) SEM image of Al_2O_3 . (b) EDS image of Al_2O_3 .

Figure 6 illustrates that the Al_2O_3 inclusions with irregular shapes are black, which do not change much with the frequency. In addition to Al_2O_3 inclusions, the number of other composite oxides, which include multiple elements, such as Al, Ca, Mg, Si, and Mn, are the largest. However, the Al content among other composite oxides in ingots is the highest, as shown in Figure 7b–f. The oxides in consumable electrodes are mainly calcium aluminate, and the Ca content in inclusions is higher than the Al content (Figure 7a). Considering that the S content in ingots is very low and the number of oxysulfides is small, they will not be discussed in this work.

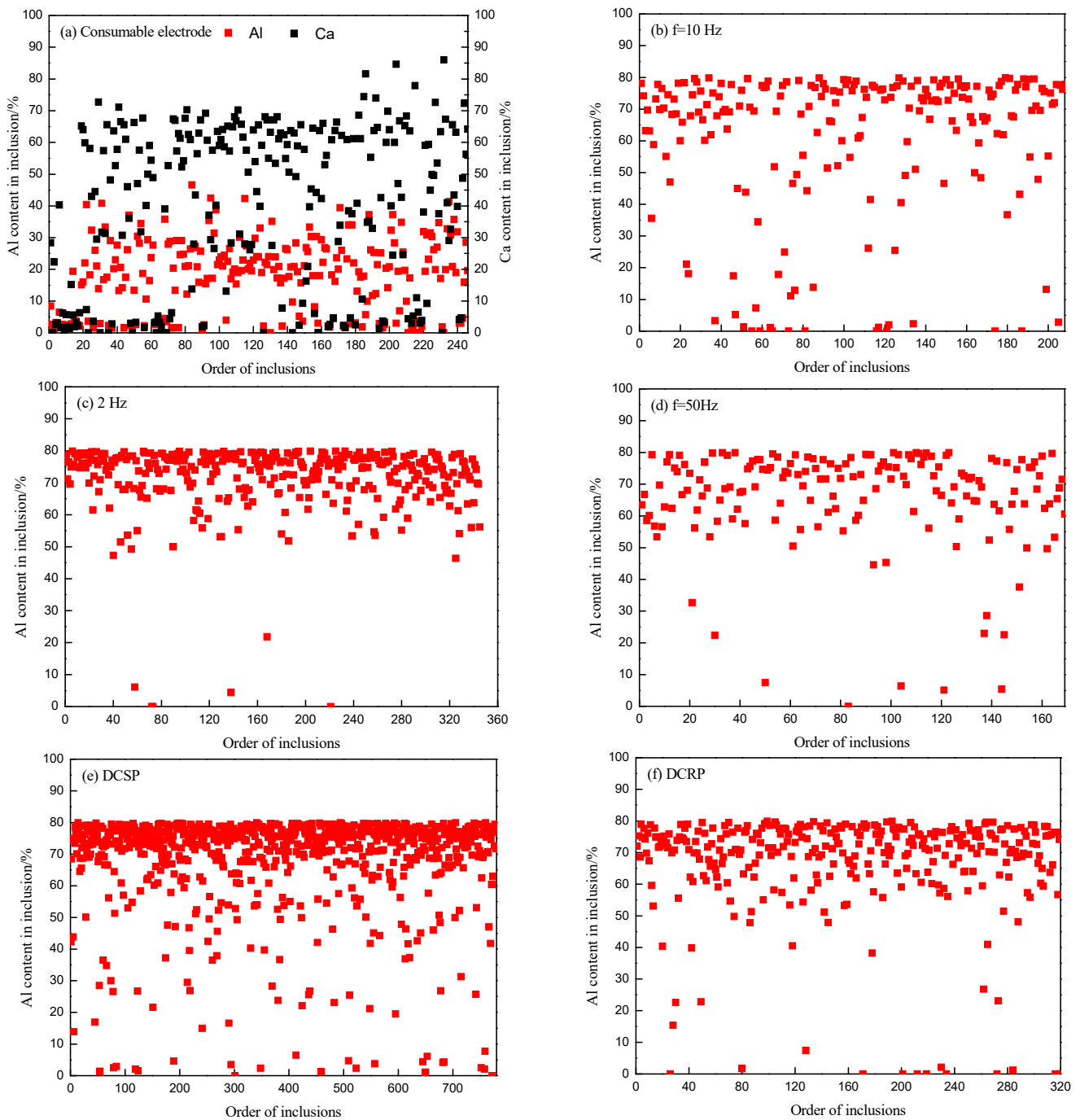


Figure 7. Composition of other composite oxide inclusions in ESR ingot.

3.2.3. Variation of Number and Size of Different Types of Inclusions

Figure 8 shows the variation in the number and size of different types of inclusions with various power supply modes.

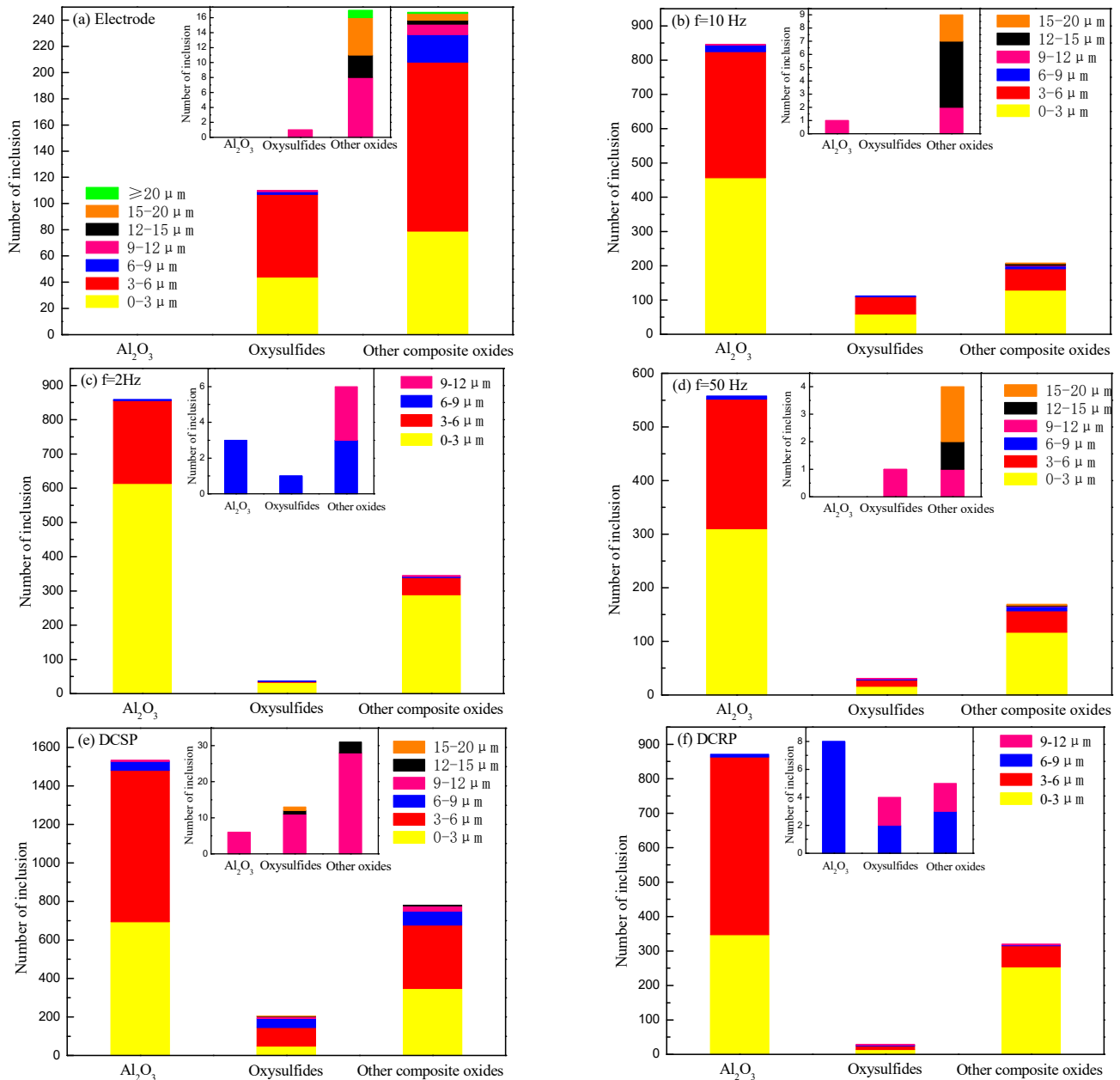


Figure 8. Variation of number and size of different types of inclusions with different power supply modes.

It can be seen from Figure 8 that regardless of the power supply modes and type of inclusions, the diameter of inclusion in ingots is mainly less than $6\ \mu\text{m}$. However, the number of large inclusion changes obviously with the change of frequency. The large inclusions in the consumable electrode are mainly calcium aluminate, and the diameter of six inclusions is larger than $15\ \mu\text{m}$. The maximum diameter of the inclusions is $27.4\ \mu\text{m}$. When the power frequency is $10\ \text{Hz}$, the diameters of all Al_2O_3 are less than $12\ \mu\text{m}$, and the diameters of oxysulfides are less than $9\ \mu\text{m}$. The diameter of other composite oxides that contain Al is larger, but the maximum diameter does not exceed $15\ \mu\text{m}$. When the power frequency decreases to $2\ \text{Hz}$, the diameter of all Al_2O_3 and oxysulfides are less than $9\ \mu\text{m}$, and the maximum diameter of other composite oxides is less than $12\ \mu\text{m}$. When the

power frequency is 50 Hz, the diameters of all Al_2O_3 are less than 9 μm , the diameter of all oxysulfides is less than 12 μm , but the maximum diameter of composite oxide is more than 15 μm . When DCSP mode is adopted, the maximum diameter of Al_2O_3 does not exceed 12 μm , the maximum diameter of oxysulfide is more than 20 μm , and the composite oxides that contain Al do not exceed 15 μm . However, the number of inclusions increases obviously. When the DCRP mode is adopted, the maximum diameter of Al_2O_3 does not exceed 9 μm . The maximum diameter of the oxysulfide and composite oxides that contain Al does not exceed 12 μm .

The above results show that regardless of the power supply modes, the diameter of Al_2O_3 in the electroslag ingot is smaller. Although the number of inclusion, especially Al_2O_3 , in electroslag ingot increases significantly, no obvious change is observed in the diameter of the inclusions.

4. Discussion

The experimental results in Section 3 show that the power supply mode has a great effect on the cleanliness of the electroslag ingot. In the electroslag remelting process, the parameters, including current, voltage, slag composition, slag amount, and atmosphere, are the same. Hence, the cleanliness of the electroslag ingot is considered directly related to the power frequency.

Notably, the frequency is the power supply parameter of the electroslag furnace, which is only the inducement for the increase in oxygen content. During the remelting process, the consumable electrode inserted in the slag pool is melted layer by layer. Therefore, the increase in oxygen content must come from the slag pool. In addition, a marked difference is observed in the Al content in electroslag ingots, as shown in Table 3.

Table 3. Chemical composition of electroslag ingots.

Experimental Schemes	Power Supply Mode	Chemical Composition/%									
		C	Si	Mn	P	S	Cr	Ni	Al	O	Ca
Electrode	/	0.019	0.411	1.175	0.037	0.0025	18.27	8.10	0.010	0.0025	0.0027
1	10 Hz	0.021	0.404	1.131	0.037	0.0027	17.92	7.86	0.028	0.0066	0.0005
2	2 Hz	0.023	0.391	1.120	0.037	0.0023	18.11	7.89	0.029	0.0076	0.0006
3	DCSP	0.030	0.393	1.121	0.038	0.0031	18.00	7.95	0.095	0.0155	0.0005
4	DCRP	0.023	0.396	1.114	0.037	0.0029	18.10	7.98	0.037	0.0100	0.0006
5	50 Hz	0.022	0.395	1.126	0.036	0.0020	18.19	8.07	0.018	0.0043	0.0005

Table 3 shows that when the different power supply modes are used for remelting, the Al content in ingots changes significantly. When the power frequency is 50 Hz, the Al content in the electroslag ingot increases to 0.018% from 0.01% in the consumable electrode. When the power frequency is 10 Hz and 2 Hz, the Al content increases to 0.028% and 0.029%, respectively. The Al content further increases to 0.037% after remelting with the DCRP power supply mode. The Al content increases sharply to 0.095% when the DCRP power supply mode is adopted. During the electroslag remelting, 30% Al_2O_3 -70% CaF_2 slag is adopted, and no Al-bearing materials are added to the slag pool. Therefore, the increase in Al in the electroslag ingot must come from Al_2O_3 in the slag pool.

In an open electroslag remelting with a power supply of 50 Hz, the oxygen content will increase inevitably, and the Al content in the electroslag ingot will decrease because of the oxidation of air [17–20]. Even if the electrode surface is polished and gas protection is used during remelting, Al content may increase slightly. However, in this experiment, the oxygen and Al contents in the electroslag ingot increase simultaneously, which should be caused by the decomposition of Al_2O_3 in the slag pool. The increase in the number of Al_2O_3 and Al-containing composite inclusions in electroslag ingot in Figures 5 and 7 further confirms this conclusion.

In the previous research, the authors study the influence of different frequencies on the oxygen and Al content in GCr15 bearing steel and 304 stainless steel electroslag ingots in detail, and the research results are consistent with the research results in this paper (as shown in Figure 9), which fully proves that the Al_2O_3 in slag pool is partially electrolyzed under the action of low frequency [16].

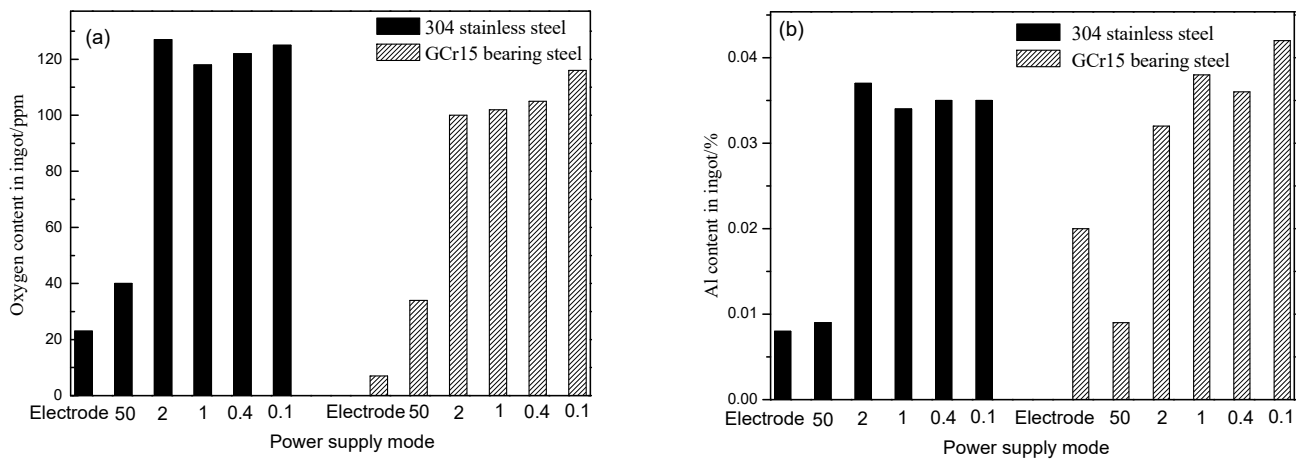
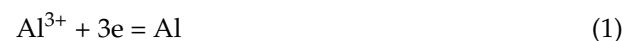


Figure 9. Oxygen and Al content in ingots with different power supply modes. ((a)—Oxygen content; (b)—Al content).

Relevant researches show that some oxides in slag in the DC electroslag remelting process will be electrolyzed, thereby resulting in the increase in oxygen content in electroslag ingot [21–23], and the results in this paper further confirm this viewpoint. When the power supply frequency is low, the DC tendency, which is very likely to electrolyze some oxides in slag, increases.

When 30% Al_2O_3 -70% CaF_2 slag is adopted, the components of slag exist in the form of Al^{3+} , Ca^{2+} , O^{2-} , F^- and AlO_3^{3-} in high-temperature slag pool [9,24]. Under the action of the high-density current, the cations move to the cathode, and anions move to the anode. According to the potential sequence of ions, Al^{3+} obtains electrons more easily than Ca^{2+} , whereas O^{2-} loses electrons more easily than F^- . Therefore, the cathode/anode reaction is expressed as follows [25].



For AlO_3^{3-} , a small amount of Al_2O_3 will be decomposed according to Formula (3) [24].



Al^{3+} obtains electrons in anions, as shown in Formula (1). AlO_3^{3-} discharges at the anode, as shown in Formula (4).



Through reactions (1)–(4), Al_2O_3 is decomposed into $[\text{Al}]$ and $[\text{O}]$ and enters the metal pool, as shown in Figure 10. However, $[\text{Al}]$ and $[\text{O}]$ do not react immediately to form Al_2O_3 inclusions but gradually form Al_2O_3 inclusions with the decrease in temperature in the metal pool, which inhibits the growth of inclusions. Therefore, even if the oxygen content and the number of inclusions in electroslag ingot increase, few large Al_2O_3 inclusions are found, as shown in Figure 8. Even if the oxygen content in the electroslag ingot is as high as 155.3 ppm when the DCSP power supply mode is adopted, the maximum diameter of Al_2O_3 inclusions is still less than 12 μm .

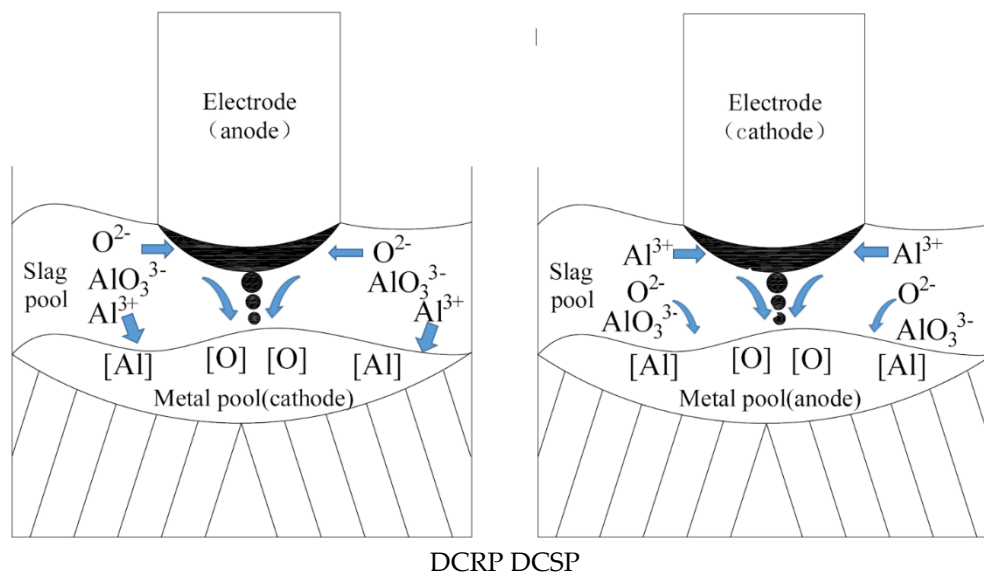


Figure 10. Schematic diagram of Al_2O_3 electrolysis.

Notably, the oxygen content in the electroslag ingot remelted by DCSP mode is more than 50% higher than that by DCRP mode. When the consumable electrode is the anode (DCRP mode), O^{2-} and AlO_3^{3-} migrate toward the anode and then lose electrons to form [O], entering the liquid metal film at the electrode cone. Given that the current density at the electrode cone is the largest, more Al_2O_3 is electrolyzed, which results in more [O] entering the metal film.

However, the [O] and [Al] in the metal film will combine again to form Al_2O_3 because of the low temperature, and part of the Al_2O_3 will be absorbed by the slag during the dropping process of the metal droplet; the oxygen content in ingot is relatively low. Al^{3+} migrates toward the cathode (slag-metal interface) and gains electrons to form [Al] entering the metal pool. The increase in Al content in the ingot is small because the [Al] in the metal film is partially oxidized to offset the increase in Al content in the metal pool caused by electrolysis.

When the consumable electrode is the cathode (DCSP mode), Al^{3+} migrates toward the cathode and then gains electrons to form [Al], entering the liquid metal film at the electrode cone. Given that the consumable electrode contains a certain amount of Al and the dissolved oxygen is very low, the loss of Al in the metal film is very small. As the film forms droplets and then drops into the metal pool, the Al content increases significantly. Both O^{2-} and AlO_3^{3-} lose electrons to form [O] entering the metal pool, and the oxygen content in the ingot also increases greatly. Therefore, compared with the DCRP power supply mode, when the DCSP mode is used for remelting, not only the oxygen content but also the Al content in the ingot increase significantly.

In addition, the current density has a great effect on the electrolysis of oxide in the slag pool. With the increase in mold diameter, the current density decreases rapidly, which generally follows the law of Formula (5) [26]:

$$\bar{J}_{\text{mold}} = \frac{260}{D_{\text{mold}}} \quad (5)$$

where \bar{J}_{mold} is the average remelting current density, A/cm^2 ; and D_{mold} is the mold diameter, cm.

Therefore, in large-scale industrial production, the electrolysis effect of low-frequency and DC power supply needs to be verified further.

5. Conclusions

In the present work, laboratory-scale electroslag remelting experiments are conducted to study the effect of power supply modes on the cleanliness of electroslag ingots. The main conclusions can be summarized as follows.

- (1) Compared with the power frequency of 50 Hz, the oxygen content in the electroslag ingot increases significantly when the frequency of 2 Hz or DC power is used. The influence order of frequency on oxygen content is DCSP, DCRP, 2 Hz, and 50 Hz. The oxygen content is the highest with DCSP mode and the lowest with the frequency of 50 Hz.
- (2) With the low-frequency and DC power supply modes, the number of inclusions in electroslag ingot increases obviously, but the increased inclusions are mainly Al_2O_3 . However, the diameter of inclusions is smaller, and the maximum diameter is not more than 20 μm .
- (3) When $\text{CaF}_2\text{-Al}_2\text{O}_3$ slag is used for electroslag remelting, the oxygen content in the electroslag ingot increases because [O] and [Al] generated by the electrolysis of Al_2O_3 enter the metal pool. However, the Al_2O_3 in the electroslag ingot is regenerated with the decrease in metal pool temperature and solidification; the inclusion size is fine.

Author Contributions: Conceptualization, L.C. and X.S.; methodology, L.C.; validation, X.S.; investigation, B.W.; writing—original draft preparation, Y.W.; writing—review and editing, X.S.; supervision, L.C.; funding acquisition, L.C. All authors have read and agreed to the published version of the manuscript.

Funding: This work was supported by the National Natural Science Foundation of China (Grant No. 52074002, 52174289, 51974002) and Natural Science Foundation of Anhui Province (Grant No. 2208085J37).

Institutional Review Board Statement: No applicable.

Informed Consent Statement: No applicable.

Data Availability Statement: No applicable.

Conflicts of Interest: The authors declare no conflict of interest.

References

1. Li, Z.B. *Electroslag Metallurgy Equipment and Technology*; Metallurgical Industry Press: Beijing, China, 2012.
2. Lv, P. Key Technology of large-tonnage electroslag furnace low frequency power supply. Master's Thesis, Xi'an Shiyou University, Xi'an, China, 2017; pp. 1–2.
3. Yu, K.; Yu, A.S.; Yang, X.J. Effect of low frequency electroslag remelting on microstructure and properties of NO8367 austenitic stainless steel. *Specail Cast. Nonferrous Alloy*. **2019**, *23*, 133–136.
4. Igizianova, N.A.; Sokolova, E.V. Modeling electromagnetic processes in direct current electroslag remelting. *Int. J. Adv. Manuf. Technol.* **2021**, *113*, 3189–3193. [[CrossRef](#)]
5. Sibaki, E.K.; Kharicha, A.; Wu, M.; Ludwig, A.; Holzgruber, H.; Omer, B.; Ramprecht, M. A numerical study on the influence of the frequency of the applied AC current on the electroslag remelting process. In *Proceedings of the International Symposium on Liquid Metal Processing and Casting, Austin, TX, USA, 22–25 September 2013*; John Wiley and Sons Inc.: Hoboken, NJ, USA, 2013; pp. 13–19.
6. Wang, H.; Zhong, Y.B.; Li, Q.; Li, W.Q.; Ren, W.L.; Lei, Z.S.; Ren, Z.M.; He, Q. Influences of the transverse static magnetic field on the droplet evolution behaviors during the low frequency electroslag remelting process. *ISIJ Int.* **2017**, *57*, 2157–2164. [[CrossRef](#)]
7. Orlov, V.; Levkov, L.; Dub, V.; Balikoev, A.; Shurygin, D. New approach to development and manufacturing technologies of duplex steel. In *Proceedings of the 1st International Conference Corrosion in the Oil and Gas Industry, Saint Petersburg, Russia, 14–16 May 2019*; EDP Sciences: Les Ulis, France, 2019.
8. Liang, Q.; Chen, X.C.; Ren, H.; Chen, C.B.; Guo, H.J. Numerical simulation of Electroslag Remelting process for producing GH4169 under different current frequency. In *Proceedings of the 3rd International Conference on Manufacturing Science and Engineering, Xiamen, China, 27–29 March 2012*; Trans Tech Publications: Zurich, Switzerland, 2012; pp. 1556–1565.
9. Jiang, Z.H.; Dong, Y.W.; Geng, X.; Liu, F.B. *Electroslag Metallurgy*; Science Press: Beijing, China, 2015.
10. Wang, Q.; Liu, Y.; Wang, F.; Li, G.Q.; Li, B.K.; Qiao, W.W. Numerical Study on the Effect of Electrode Polarity on Desulfurization in Direct Current Electroslag Remelting Process. *Metall. Mater. Trans. B* **2017**, *48*, 2649–2663. [[CrossRef](#)]
11. Aksenov, I.A.; Matveeva, M.A.; Chumanov, I.V. Influence of the ESR Parameters on the Removal of Sulfur. *Russ. Metall.* **2019**, *2019*, 601–607. [[CrossRef](#)]
12. Parr, A.; Schneider, R.; Zeller, P.; Reiter, G.; Paul, S.; Wuerzinger, P. Effect of electrical parameters on type and content of non-metallic inclusions after electro-slag-remelting. *Steel Res. Int.* **2014**, *85*, 570–578. [[CrossRef](#)]

13. Parr, A.; Schneider, R.; Zeller, P.; Reiter, G.; Paul, S.; Silier, I.; Wuerzinger, P. Influence of the polarity on the cleanliness and the inclusion types in the ESR process. In *Proceedings of the International Symposium on Liquid Metal Processing and Casting (LMPC2013)*, Austin, TX, USA, 22–25 September 2013; John Wiley and Sons Inc.: Hoboken, NJ, USA, 2013; pp. 29–36.
14. Mitchell, A. Electrochemical Aspects of the ESR Process. In *Proceedings of the International Symposium on Liquid Metal Processing and Casting (LMPC2015)*, Leoben, Austria, 20–24 September 2015; Institute of Physics Publishing: Bristol, UK, 2015.
15. Chang, L.Z.; Shi, X.F.; Yang, H.S.; Li, Z.B. Effect of low-frequency AC power supply during electroslag remelting on qualities of alloy steel. *J. Iron Steel Res. Int.* **2009**, *16*, 7–11. [[CrossRef](#)]
16. Chang, L.Z.; Su, Y.L.; Zhang, L.F.; Zhu, C.L.; Xu, T.; Shi, X.F. Influence of power frequency on cleanliness of electroslag ingot during electroslag remelting process. *Iron Steel* **2022**, *57*, 43–53.
17. Hou, D.; Jiang, Z.H.; Qu, T.P.; Wang, D.Y.; Liu, F.B.; Li, H.B. Aluminum, titanium and oxygen control during electroslag remelting of stainless steel based on thermodynamic analysis. *J. Iron Steel Res. Int.* **2019**, *26*, 20–31. [[CrossRef](#)]
18. Shi, C.B.; Wang, S.J.; Li, J.; Cho, J.W. Non-metallic inclusions in electroslag remelting: A review. *J. Iron Steel Res. Int.* **2021**, *28*, 1483–1503. [[CrossRef](#)]
19. Duan, S.C.; Shi, X.; Wang, F.; Zhang, M.C.; Sun, Y.; Guo, H.J.; Guo, J. A Review of Methodology Development for Controlling Loss of Alloying Elements During the Electroslag Remelting Process. *Metal. Mater. Tran. B* **2019**, *50*, 3055–3071. [[CrossRef](#)]
20. Zhou, D.G.; Chen, X.C.; Fu, J.; Wang, P.; Li, J.; Xu, M.D. Inclusion in electroslag remelting and continuous casting bearing steels. *J. Univ. Sci. Technol. Beijing* **2000**, *22*, 26–30.
21. Kawakami, M.; Takenaka, T.; Ishikawa, M. Electrode reactions in DC electroslag remelting of steel rod. *Ironmak. Steelmak.* **2002**, *29*, 287–292. [[CrossRef](#)]
22. Kato, M.; Hasegawa, K.; Nomura, S.; Inouye, M. Transfer of oxygen and sulfur during direct-current electroslag remelting. *Trans. Iron Steel Inst. Jpn.* **1983**, *23*, 618–627. [[CrossRef](#)]
23. Karimi-Sibaki, E.; Kharicha, A.; Wu, M.H.; Ludwig, A.; Bohacek, J. Toward Modeling of Electrochemical Reactions during Electroslag Remelting (ESR) Process. *Steel Res. Int.* **2017**, *88*, 1700011. [[CrossRef](#)]
24. Jiang, H.Y. *Metallurgical Electrochemistry*; Metallurgical Industry Press: Beijing, China, 1983.
25. Wang, J. *Electrolytic Aluminum Production Process and Equipment*; Metallurgical Industry Press: Beijing, China, 2006.
26. Li, Z.B. *Electroslag Metallurgy Theory and Practice*; Metallurgical Industry Press: Beijing, China, 2010.

Disclaimer/Publisher’s Note: The statements, opinions and data contained in all publications are solely those of the individual author(s) and contributor(s) and not of MDPI and/or the editor(s). MDPI and/or the editor(s) disclaim responsibility for any injury to people or property resulting from any ideas, methods, instructions or products referred to in the content.